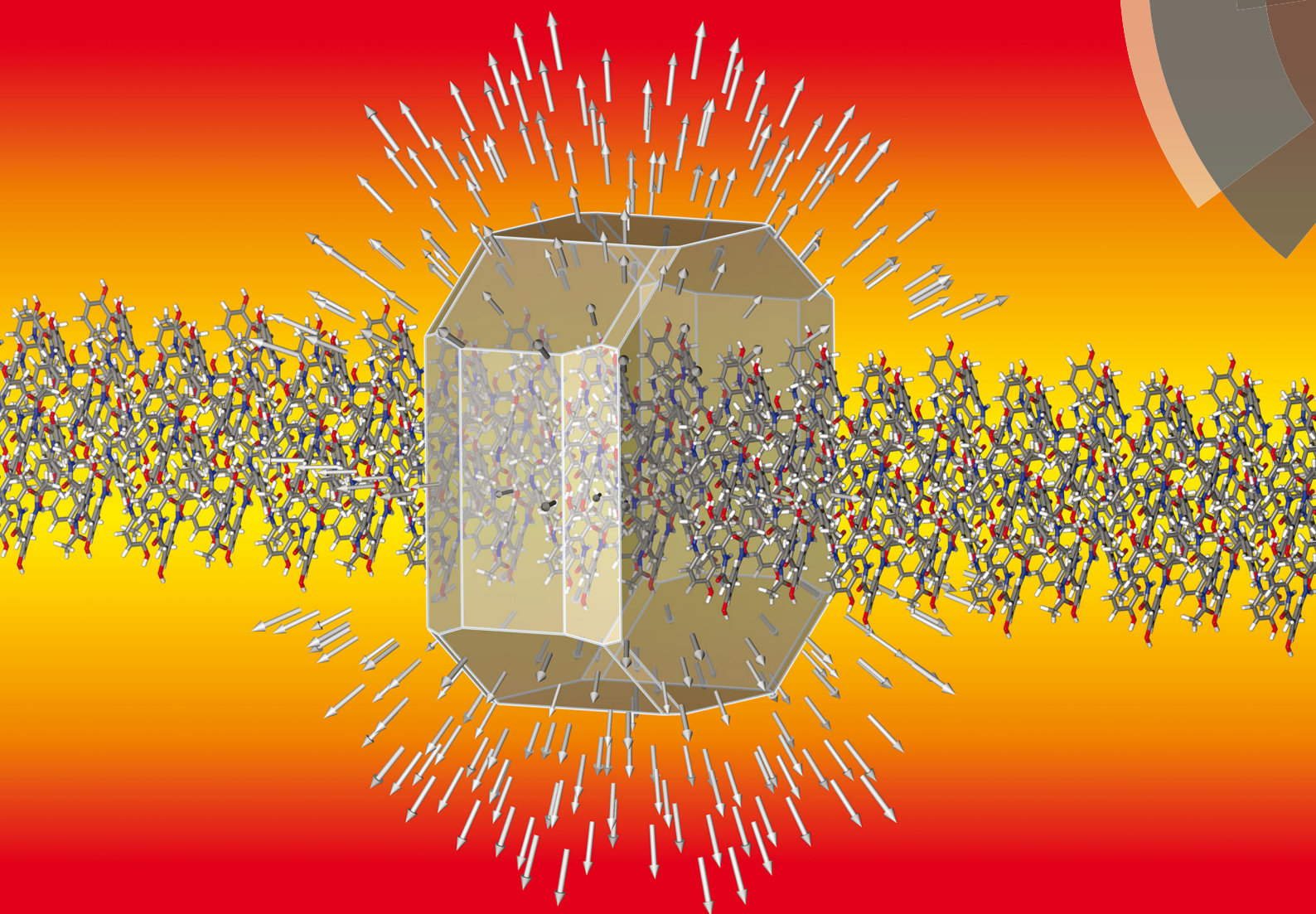


# ChemComm

Chemical Communications

[www.rsc.org/chemcomm](http://www.rsc.org/chemcomm)



ISSN 1359-7345



COMMUNICATION

Ian J. Scowen *et al.*

Stabilisation of metastable polymorphs: the case of paracetamol form III

**175** YEARS



Cite this: *Chem. Commun.*, 2016, 52, 12028

Received 15th June 2016,  
Accepted 5th August 2016

DOI: 10.1039/c6cc05006a

[www.rsc.org/chemcomm](http://www.rsc.org/chemcomm)

## Stabilisation of metastable polymorphs: the case of paracetamol form III†

Richard Telford,<sup>a</sup> Colin C. Seaton,<sup>a</sup> Alexander Clout,<sup>b</sup> Asma Buanz,<sup>b</sup> Simon Gaisford,<sup>b</sup> Gareth R. Williams,<sup>b</sup> Timothy J. Prior,<sup>c</sup> Chidera H. Okoye,<sup>d</sup> Tasnim Munshi<sup>d</sup> and Ian J. Scowen<sup>\*d</sup>

**The design of a melt synthesis of the first air-stable formulation of the metastable form III of paracetamol is derived from thermo-spectroscopic and thermo-diffraction experiments. Melt crystallisation in the presence of  $\beta$ -1,4-saccharides produces form III selectively and the excipients appear to act as stabilising 'active' templates of the metastable polymorph.**

Accessing and stabilising metastable polymorphic forms of active pharmaceutical ingredients remains a major challenge in pharmaceutical product innovation.<sup>1,2</sup> While systemic approaches to polymorphic diversity in organic solids remain elusive, we report here studies into the polymorphism of paracetamol that indicates a promising role for the 'excipient' matrix to direct and stabilise metastable forms and the importance of *in situ* characterisation of polymorphism for formulation design.

Paracetamol exists in three polymorphic forms; a stable phase (I) and two metastable phases (II, III). Form I packs with a herringbone motif, while forms II and III display layered structures.<sup>3,4</sup> The structure of form I results in poor compactibility, leading to poor tablet quality.<sup>3</sup> However, difficulties in producing suitable quantities of either form II or III have limited research into their physical properties. While form III has been reported as highly unstable in air, even being referred to as 'elusive',<sup>4</sup> recent reports indicate that surfaces such as glass<sup>5</sup> and silica<sup>6</sup> can promote its growth, and careful control of heating and cooling rates during melt crystallisation have also been demonstrated to lead to form III.<sup>7,8</sup> Additionally, inclusion of hydroxypropyl methylcellulose (HPMC) into the paracetamol melts can

alter the kinetics of the crystallisation of the two metastable phases, which provides an initial insight into the use of polysaccharides as templating agents.<sup>9,10</sup>

We report here the first air-stable formulations of paracetamol form III based on an apparently active interaction with an excipient matrix derived from saccharides. *In situ* spectroscopic and diffraction studies have offered unique insight into the melt synthesis. Furthermore, this approach is shown to be amenable to scale up.

The addition of molecular additives to alter the kinetics of the crystallisation process to obtain metastable polymorphs has been a frequent topic of study.<sup>11,12</sup> The inhibition of the stable phase through preferential interactions between the additive and the surface available functional groups of the crystal may lead to slowing of crystal growth,<sup>13–17</sup> while preferential interaction of the additive with the unstable phase may lead to stabilisation of the phase or alter the balance of the kinetic rates of the two phases.<sup>17</sup> Design or selection of a suitable additive may then be used to control the crystallisation processes and tailor the creation of a desired polymorph.

Melt synthesis of air-stable form III utilises the sugar-based excipients lactose monohydrate and HPMC. The crystallisation process has been followed with simultaneous Raman-DSC and time-resolved X-ray diffraction-DSC experiments. Critically, computational modelling of the interfacial interactions at the predicted major faces of the respective paracetamol crystals and the excipient indicate significant drivers to the stabilisation of form III through hydrogen bonding.

Samples of paracetamol and an excipient (10% w/w) were subjected to heating and cooling cycles with the phase of the crystal established with *in situ* Raman spectroscopy throughout the heating cycles.‡ A standardised heating cycle was implemented: (i) ambient to 180 °C at 10 °C min<sup>-1</sup> and held for 2 minutes to melt the paracetamol and excipient mixture; (ii) quench cooling to 0 °C to generate an amorphous phase; (iii) reheating to 180 °C at 10 °C min<sup>-1</sup>. This last cycle caused three major thermal events: an exotherm at *ca.* 90 °C corresponding to crystallisation [identified as form III with indicative Raman shifts of

<sup>a</sup> School of Chemistry and Forensic Sciences, University of Bradford, Richmond Road, Bradford, BD7 1DP, UK

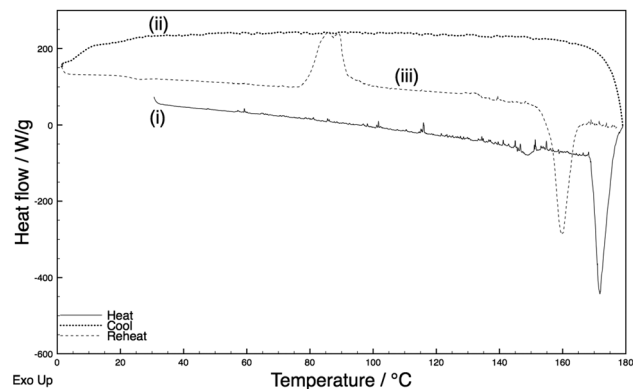
<sup>b</sup> UCL School of Pharmacy, University College London, 29-39 Brunswick Square, London WC1N 1AX, UK

<sup>c</sup> Department of Chemistry, University of Hull, Cottingham Road, Hull, HU6 7RX, UK

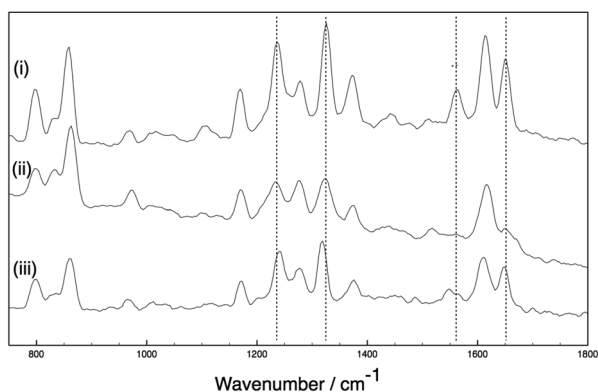
<sup>d</sup> School of Chemistry, University of Lincoln, Lincoln LN6 7DL, UK.  
E-mail: [iscowen@lincoln.ac.uk](mailto:iscowen@lincoln.ac.uk)

† Electronic supplementary information (ESI) available: DSC and Raman spectra for all systems. Predicted morphologies for form I and III. See DOI: 10.1039/c6cc05006a





(a)



(b)

**Fig. 1** (a) DSC thermograms and (b) Raman spectra recorded at (i) 30 °C before heating [form I], (ii) 30 °C after quench cooling [amorphous] and (iii) 110 °C [form III] after reheating for a 10% lactose containing sample of paracetamol (annotated with key spectral shifts observed from I to III).

phenyl C–C (*ca.* 1620  $\text{cm}^{-1}$ ), amide II (*ca.* 1560  $\text{cm}^{-1}$ ), and phenyl ring deformations (*ca.* 1320 and 1230  $\text{cm}^{-1}$  bands),<sup>8,18</sup> a second exotherm at 133 °C (conversion to form II), followed by an endotherm at 160 °C (melt of form II) (Fig. 1). The system with HPMC shows essentially identical behaviour (ESI,<sup>†</sup> Fig. S1 *cf.* Fig. S2). By comparison, an excipient free sample (ESI,<sup>†</sup> Fig. S3) melts on heating and cools to an amorphous phase. Upon reheating, recrystallisation to form II occurs at *ca.* 83 °C before the system melts at *ca.* 159 °C – importantly, no exotherm is apparent at 133 °C.

A parallel study of the melt synthesis of form III with lactose was undertaken using hyphenated *in situ* X-ray diffraction/DSC, using similar protocols to those in DSC-Raman studies.<sup>§</sup> Due to a difference in the quenching rate, this sample results in a mixture of amorphous/form II paracetamol at room temperature as shown by the presence of Bragg reflections in the sample (Fig. 2, top). Upon reheating of this sample, the DSC shows a broad exotherm with a maximum at *ca.* 85 °C, followed by a second exotherm at 130 °C and an endotherm at just below 160 °C. The latter corresponds to the melt of form II, and XRD patterns collected above this temperature show no diffraction features. The two exotherms correspond to distinct changes in the XRD patterns. The first exotherm coincident with the

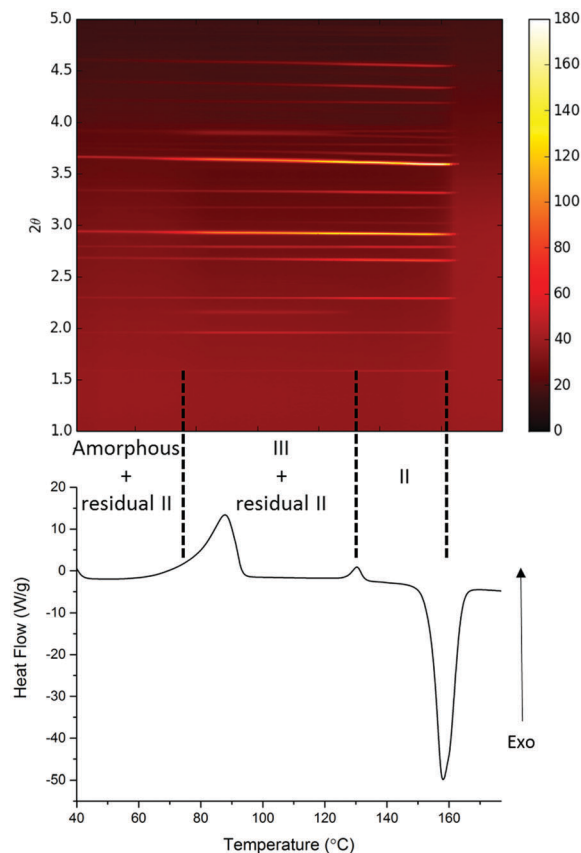


**Fig. 2** Simultaneous XRD (top)-DSC (bottom) data collected on a sample of paracetamol/lactose. The sample was heated to 180 °C, held at this temperature for 2 min, and quenched before a second heating cycle performed at 10 °C  $\text{min}^{-1}$ . The data shown are for this second heat.

crystallisation of form III from the amorphous material present. The second exotherm corresponds to the conversion of form III present into form II, resulting in a pure form II above 130 °C which persists until the mixture melts. Each pattern was analysed using the Rietveld method (selected datasets are given in the ESI,<sup>†</sup> Fig. S4 and Table S1). The presence of form II throughout the experiment up to the melting point is clear, as is the fact that form III grows in during the first exotherm and is converted to form II at the second. The area under the diffraction pattern from each phase was calculated (ESI,<sup>†</sup> Fig. S5). It is clear that the amount of form III present is largely constant between the two exotherms, despite the fact that form II crystals are also present. The amount of form II present increases throughout the experiment until the second exotherm, presumably a result of seeding of crystallisation from the amorphous material (in contrast to the pure phase III inferred from the Raman-DSC experiment in this region of the thermogram). Thus the lactose additive is still able to stabilise form III even in the presence of form II crystals.

Interactions between the sugar excipients (modelled as lactose) and paracetamol were investigated computationally,<sup>¶</sup> through the minimisation of the intermolecular interactions between crystal surfaces of the differing paracetamol polymorphs and a lactose molecule. For forms I and III, the dominant crystal



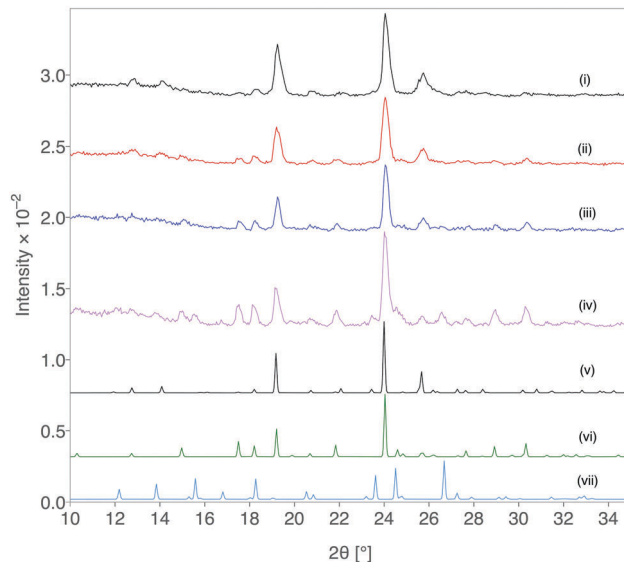
**Table 1** Calculated interaction energies for lactose with paracetamol surfaces

System	Energy (kJ mol <sup>-1</sup> )
Form I (001 surface)	-42.748
Form I (011 surface)	-51.321
Form III (001 surface)	-55.693
Form III (010 surface)	-57.735

faces of each phase, as indicated by several morphology prediction methods<sup>||</sup> were investigated. For a single lactose molecule, significantly stronger interactions are indicated with the surfaces of form III compared to form I (Table 1). Visualisation of the strongest interactions for both systems (Fig. 3) shows that the match between hydrogen bond groups on each system is greater for form III compared to form I. It appears that the repeat of the location of the OH groups on this surface matches the lactose molecule ensuring a number of hydrogen bonds can be formed between the two systems. This matching of system size and orientation of hydrogen bonding functional groups may be the source of the stabilisation of form III and points to an active role for the excipient in stabilising the metastable form.

The creation of form III was successfully scaled up using this approach and 100 mg quantities have been reproducibly obtained with the lactose monohydrate system.<sup>\*\*</sup> The stability of the obtained formulation was characterised by XRD immediately after formation and at periods throughout storage under standard ambient conditions for greater than 12 months (Fig. 4). After 12 months, form III shows partial transformation to other forms, but remarkably there was retention of form III over this time scale.

The design of an air-stable formulation for paracetamol form III has been developed with hyphenated thermo-spectroscopic and thermo-diffraction experiments. Scale-up of the process yields

**Fig. 4** Comparison of XRD patterns for paracetamol form III formulation at (i) 0 days, (ii) 15 days, (iii) 32 days, (iv) 12 months and the simulated XRD patterns for (v) form III, (vi) form II and (vii) form I.

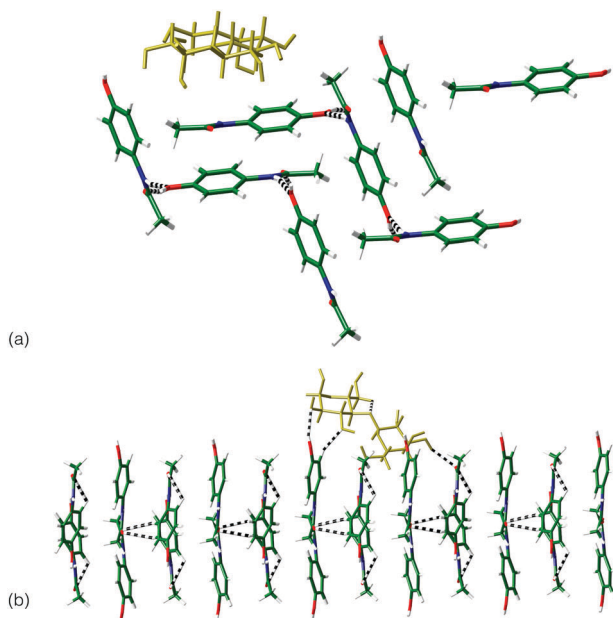
material that shows long-term stability for form III and is obtainable reproducibly, albeit in a mixture with other forms (for example, form II). Crucially, a match between the size of the sugar excipient molecule and functional group types of the surfaces of the form III crystals appears to be a major contribution to this stability. Therefore, an 'active' excipient template that stabilises solid state forms inaccessible under ambient conditions underpins this work. We aim to extend this approach and further develop predictive computational tools that offer a new approach in designing formulations of metastable forms in the future.

We thank Diamond Light Source for access to beamline I12 (EE-12735) the results from which contributed to the results presented.

## Notes and references

‡ DSC data were collected using TA Instruments Q2000 DSC with a RCS 90 cooling system with the samples run in open  $T_{zero}$  aluminium pans. Approximately 6 mg of sample was used and each experiment was run in duplicate. This was coupled with a Renishaw Portable Raman Analyzer RX210 (785 nm laser, 100% laser power, 1 accumulation, 3 seconds exposure time) for the *in situ* DSC-Raman analysis. The optical probe of the system was held approximately 3 cm from the sample and a photo calorimetry accessory was used in place of the DSC lid to allow access to the sample but retaining accurate temperature control. During each DSC cycle, Raman spectra were collected every 3 °C. Powder X-ray diffraction data were collected using a Bruker D8 diffractometer in Bragg-Brentano  $\theta$ - $\theta$  geometry with Cu K $\alpha$  radiation (1.5418 Å) with a scintillation counter. Data were collected in the  $2\theta$  range 5 to 40° in steps of 0.05° with a 6 second count time.

§ *In situ* XRD-DSC was undertaken using Beamline I12 of the Diamond Light Source. Full details of the apparatus will be reported elsewhere.<sup>19</sup> In brief, a TA Instruments Q20 calorimeter was modified by drilling two holes in the furnace head to permit the X-ray beam to penetrate it. Samples of paracetamol/lactose (90/10 w/w, total mass *ca.* 20 mg) were then heated at 10 °C min<sup>-1</sup> as for DSC-Raman work and 4 s diffraction patterns collected on a Thales Pixium RF4343 detector every 6 s. DSC data were analysed using the TA Instruments Universal Analysis

**Fig. 3** Comparison of the interaction between lactose molecule (yellow) and: (a) (011) surface of form I; (b) the (010) surface of form III.

software, and XRD data using in-house routines. Rietveld refinements were performed using the GSAS and Topas Academic programmes.<sup>20</sup>

¶ The molecular modelling was carried out using the in-house program DEX.<sup>21–23</sup> The crystal structures of paracetamol polymorphs (form I (HXACAN30),<sup>24</sup> form II (HXACAN31)<sup>24</sup> and form III (HXACAN29),<sup>4</sup>) were extracted from the CSD,<sup>25</sup> energy minimised using the downhill simplex routine with in-house code using the potential described by No *et al.*<sup>26</sup> using atomic point charges fitted to the electrostatic potential calculated for the isolated molecules in the program orca (mpW2PLYP-D3/def2-TZVPPD).<sup>27–29</sup> The interaction energy between the crystal surface and a probe molecule was calculated in the same way and minimised using the differential evolution (DE) optimisation algorithm<sup>30,31</sup> by alteration of the position and orientation of the probe molecule on the selected crystal surface. The parameters were constrained to lie in the range  $-5$  to  $5$  Å for translations and  $-180$  to  $180^\circ$  for the rotations. The control parameters for the DE algorithm ( $K$ ,  $F$ ,  $G_{\max}$ ,  $N_p$ ) were set to 0.75, 0.75, 2000, 60. The underlying crystal surface was generated by slicing a  $3 \times 3 \times 3$  crystal block through the selected surface removing a  $3 \times 3$  layer.

|| Morphology predictions were carried out using BFDH and attachment energy methods. Dreiding and COMPASSII force fields were used with the relevant optimised crystal structure. Atomic point charges for the Dreiding force field were taken from the electrostatic fit carried out for the subsequent modelling. Resulting morphologies are presented in ESI.†

\*\* Production of form III at 100 mg scale was achieved by preparing a physical mix of form I paracetamol and lactose monohydrate (10% w/w) on a glass coverslip. This was subjected to a standard heating cycle (ambient to  $180^\circ\text{C}$  at  $10^\circ\text{C min}^{-1}$  (2 minute isotherm), followed by quench cooling to  $0^\circ\text{C}$  and reheating to  $110^\circ\text{C}$  at  $10^\circ\text{C min}^{-1}$ ) in the cell in DSC.

- 1 A. Llinas and J. M. Goodman, *Drug Discovery Today*, 2008, **13**, 198–210.
- 2 D. Mangin, F. Puel and S. Veessler, *Org. Process Res. Dev.*, 2009, **13**, 1241–1253.
- 3 G. Nichols and C. S. Frampton, *J. Pharm. Sci.*, 1998, **87**, 684–693.
- 4 M.-A. Perrin, M. A. Neumann, H. Elmaleh and L. Zaske, *Chem. Commun.*, 2009, 3181–3183.
- 5 P. Di Martino, P. Conflant, M. Drache, J. P. Huvenne and A. M. Guyot-Hermann, *J. Therm. Anal.*, 1997, **48**, 447–458.
- 6 H. M. A. Ehmann and O. Werzer, *Cryst. Growth Des.*, 2014, **14**, 3680–3684.
- 7 J. C. Burley, M. J. Duera, R. S. Steina and R. M. Vrcelj, *Eur. J. Pharm. Sci.*, 2007, **31**, 271–276.
- 8 J. B. Nanubolu and J. C. Burley, *Mol. Pharmaceutics*, 2012, **9**, 1544–1558.

- 9 A. Rossi, A. Savioli, M. Bini, D. Capsoni, V. Massarotti, R. Bettini, A. Gazzaniga, M. E. Sangalli and F. Giordano, *Thermochim. Acta*, 2003, **406**, 55–67.
- 10 S. Gaisford, A. B. M. Buanz and N. Jethwa, *J. Pharm. Biomed. Anal.*, 2010, **53**, 366–370.
- 11 R. J. Davey, K. Allen, N. Blagden, W. I. Cross, H. Lieberman, M. J. Quayle, S. Righini, L. Seton and G. J. T. Tiddy, *CrystEngComm*, 2002, 257–264.
- 12 J. Bernstein, *Polymorphism in Molecular Crystals*, Oxford University Press, 2007.
- 13 E. Staab, L. Addadi, L. Leiserowitz and M. Lahav, *Adv. Mater.*, 1990, **2**, 40–43.
- 14 R. Hiremath, S. Varney and J. Swift, *Chem. Commun.*, 2004, 2676–2677.
- 15 E. H. Lee, S. R. Byrn and M. T. Carvajal, *Pharm. Res.*, 2006, **23**, 2375–2380.
- 16 A. D. Gift, P. E. Luner, L. Luedeman and L. S. Taylor, *J. Pharm. Sci.*, 2008, **97**, 5198–5211.
- 17 R. Dowling, R. J. Davey, R. A. Curtis, G. Han, S. K. Poornachary, P. S. Chow and R. B. H. Tan, *Chem. Commun.*, 2010, **46**, 5924.
- 18 J. F. Kauffman, L. M. Batykefer and D. D. Tuschel, *J. Pharm. Biomed. Anal.*, 2008, **48**, 1310–1315.
- 19 A. Clout, A. B. M. Buanz, T. J. Prior, C. Reinhard, Y. Wu, D. O'Hare, G. R. Williams and S. Gaisford, *Anal. Chem.*, 2016, submitted.
- 20 A. C. Larson and R. B. Von Dreele, "General Structure Analysis System (GSAS)", Los Alamos National Laboratory Report LAUR 86-748, 1994.
- 21 C. C. Seaton and N. Blagden, *ACA Trans.*, 2004, **39**, 90–102.
- 22 A. Munroe, D. M. Croker, B. K. Hodnett and C. C. Seaton, *CrystEngComm*, 2011, **13**, 5903–5907.
- 23 R. J. Davey, G. Sadiq, C. C. Seaton, R. G. Pritchard, G. Coquerel and C. Rougeot, *CrystEngComm*, 2014, **16**, 4377–4381.
- 24 Y. V. Nelyubina, I. V. Glukhov, M. Yu. Antipin and K. Lyssenko, *Chem. Commun.*, 2010, **46**, 3469.
- 25 C. R. Groom, I. J. Bruno, M. P. Lightfoot and S. C. Ward, *Acta Crystallogr., Sect. B: Struct. Sci., Cryst. Eng. Mater.*, 2016, **72**, 171–179; F. H. Allen, *Acta Crystallogr., Sect. B: Struct. Sci.*, 2002, **58**, 380–388.
- 26 K. T. No, O. Y. Kwon, S. Y. Kim, K. H. Cho, C. N. Yoon, Y. K. Kang, K. D. Gibson, M. S. Jhon and H. A. Scheraga, *J. Phys. Chem.*, 1995, **99**, 13019–13027.
- 27 D. Rappoport and F. Furche, *J. Chem. Phys.*, 2010, **133**, 134105.
- 28 S. Grimme, S. Ehrlich and L. Goerigk, *J. Comput. Chem.*, 2011, **32**, 1456–1465.
- 29 S. Grimme, J. Antony, S. Ehrlich and H. Krieg, *J. Chem. Phys.*, 2010, **132**, 154104.
- 30 R. Storn and K. V. Price, *J. Global Optim.*, 1997, **11**, 341–359.
- 31 K. V. Price, R. Storn and J. Lampinen, *Differential Evolution: A Practical Approach to Global Optimization*, Springer, London, UK, 2006.

